

# UC Berkeley

## UC Berkeley Previously Published Works

**Title**

Nodal signalling is involved in left-right asymmetry in snails

**Permalink**

<https://escholarship.org/uc/item/7hp5z7dw>

**Journal**

Nature, 457(7232)

**ISSN**

0028-0836

**Authors**

Grande, Cristina

Patel, Nipam H

**Publication Date**

2009-02-01

**DOI**

10.1038/nature07603

Peer reviewed

## Nodal signaling is involved in left-right asymmetry in snails

Cristina Grande<sup>1</sup> and Nipam H. Patel<sup>1,2</sup>

<sup>1</sup>Dept. of Molecular and Cell Biology, Dept. of Integrative Biology, and Center for Integrative Genomics, University of California, Berkeley, California. 94720-3200, USA

<sup>2</sup>Howard Hughes Medical Institute

### Abstract

Many animals display specific internal or external features with left-right asymmetry. In vertebrates, the molecular pathway that leads to this asymmetry utilizes the signaling molecule Nodal, a member of the TGF- $\beta$  superfamily 1, that is expressed in the left lateral plate mesoderm 2, and loss of *nodal* function produces a randomization of the left-right asymmetry of visceral organs 3,4. Orthologs of *nodal* have also been described in other deuterostomes, including ascidians and sea urchins 5-6, but no *nodal* ortholog has been reported in the other two main clades of Bilateria: Ecdysozoa (including flies and nematodes) and Lophotrochozoa (including snails and annelids). Here we report the first evidence for a *nodal* ortholog in a non-deuterostome group. We isolated *nodal* and *Pitx* (one of the targets of Nodal signaling) in two species of snails and found that the side of the embryo that expresses *nodal* and *Pitx* is related to body chirality: both genes are expressed on the right side of the embryo in the dextral (right handed) species *Lottia gigantea* and on the left side in the sinistral (left handed) species *Biomphalaria glabrata*. We pharmacologically inhibited the Nodal pathway and found that *nodal* acts upstream of *Pitx*, and that some treated animals developed with a loss of shell chirality. These results suggest that the involvement of the Nodal pathway in left-right asymmetry might have been an ancestral feature of the Bilateria.

---

Asymmetric expression and action of the Nodal pathway is a conserved feature of deuterostomes, with *nodal* and its target gene *Pitx* acting on the left side of the embryo in chordates but on the right side in echinoderms (sea urchins) 7. Until now, the lack of identified *nodal* orthologs in the genomes of cnidarians and Ecdysozoans suggested that *nodal* evolved in an ancestor within the early deuterostome lineage. Furthermore, although the molecular pathways involved in several asymmetries in flies and nematodes are being actively investigated, so far the Nodal pathway does not seem to be involved. The third main group of Bilateria, the Lophotrochozoa, which includes snails and annelids, also displays

---

Users may view, print, copy, and download text and data-mine the content in such documents, for the purposes of academic research, subject always to the full Conditions of use:[http://www.nature.com/authors/editorial\\_policies/license.html#terms](http://www.nature.com/authors/editorial_policies/license.html#terms)

Correspondence and requests for materials should be addressed to N.H.P. (e-mail: [nipam@uclink.berkeley.edu](mailto:nipam@uclink.berkeley.edu)).

**Author contributions** CG performed experiments; CG and NHP designed experiments, collected and analyzed data, and wrote the manuscript.

**Author Information** *Nodal*, *Pitx*, and *hedgehog* sequences of *L. gigantea* and *B. glabrata* are deposited at the EMBL-GenBank data libraries; accession numbers EU394708 and EU394707 (for *nodal*), EU797117 and EU797116 (for *Pitx*) and EU394706 and EU394705 (for *hedgehog*). In addition, a *brachyury* sequence of *L. gigantea* is deposited as accession number EU797118. Reprints and permissions information is available at [npg.nature.com/reprintsandpermissions](http://npg.nature.com/reprintsandpermissions).

morphological asymmetries. One of the asymmetries that has particularly intrigued researchers is snail chirality, which refers to the body handedness and direction of shell coiling (Fig. 1). Dextral (right handed) and sinistral (left handed) forms can be found at many taxonomic levels (Fig. 1a,b), although the majority of extant snail species are dextral 8. Body chirality can be related to a much earlier chirality that is seen in all gastropod embryos, namely the chirality of the spiral cleavage pattern seen at the transition from the 4 to 8-cell embryo (Fig. 1c). For some species, both chiral forms exist within a population (Fig. 1b), and body handedness is determined by a single locus that functions maternally to determine the chirality of offspring 9-11.

To gain insight into the molecular pathway for left-right asymmetry in gastropods we investigated some of the previously described genes critical for left-right determination in other organisms. Specifically, we focused on members of the Nodal pathway in two species of snails which differ in chirality: the sinistral species *Biomphalaria glabrata* (Fig. 1d), an intermediate host for the pathogen that causes schistosomiasis, and the dextral species *Lottia gigantea* (Fig. 1e), whose complete genome sequence is assembled. We first found in *L. gigantea* several components of the Nodal signaling pathway, including *nodal* itself as well as one of the known target genes of *nodal*, the paired homeobox gene *Pitx*. We subsequently characterized cDNAs encoding proteins related to Nodal and *Pitx* in both *L. gigantea* and *B. glabrata*. Bayesian phylogenetic analyses confirmed, with high statistical support, that these potential orthologs of Nodal are indeed more closely related to deuterostome Nodal than to any other TGF- $\beta$  family member (Supplementary Figs. 1a and 2). To determine if *nodal* is also present in other lophotrochozoans, we also identified a potential ortholog of *nodal* in the annelid, *Capitella species I.*, and further phylogenetic analyses confirmed the close relationship between this sequence and gastropod and deuterostome Nodal proteins (Supplementary Fig. 1a and 2). In addition, a single potential ortholog of *Pitx* was identified in both snail species (Supplementary Fig. 1b).

We then examined the expression pattern of *nodal* and *Pitx* in both *L. gigantea* and *B. glabrata*. Snail embryos undergo indirect development, producing first a trochophore then a veliger larva. We first examined the trochophore stage, as the anterior-posterior and dorsal-ventral axes at this time are morphologically clear, and found that both genes were expressed in left-right asymmetric patterns (Figure 2). In *L. gigantea*, there are two ectodermal domains of *nodal* expression on the right side of the embryo, one cephalic region plus a lateral domain near where shell formation initiates (Fig 2a-d). In *B. glabrata*, expression is seen in an ectodermal region on the left side of the embryo near where the shell gland will form in the posterior midline region (Fig. 2e-h). In the veliger stage of *B. glabrata* an additional domain in the left cephalic ectoderm is seen (Supplementary Fig. 3). To confirm the right versus left expression, we double-labeled embryos of both species for *nodal* and *hedgehog*, a gene that is expressed at the ventral midline in snails (Fig. 2i-l) 12.

At the trochophore stage of *L. gigantea*, *Pitx* expression is seen in a group of ectodermal cells on the right side of the larvae, adjacent to those that express *nodal*, as well as in the developing gut (Fig. 2m-n; Fig. 3i-j). At later stages, *Pitx* expression is maintained in these domains but becomes visible as well in the right cephalic ectoderm, and in a symmetric domain of the visceral mass (Supplementary Fig. 4). In the trochophore of *B. glabrata*, *Pitx*

expression is observed in the ectoderm on the left side of the larvae close to the shell gland and adjacent to the group of cells that express *nodal*, as well as in symmetric patterns in the stomodeum and gut (Fig. 2o-p). Later in development, *Pitx* is also symmetrically expressed in the developing cephalic tentacles (Supplementary Fig. 4).

We next examined earlier stages of development to determine when the asymmetric patterns were first visible. In both species, *nodal* transcripts were first detected at the 32-cell stage (Fig. 3a, c). The bilateral axis is visible in snails at the 32 to 64-cell stage, when 3D produces mesentoblast 4d which subsequently divides in a bilateral fashion to form paired stem cells that will give rise to the mesodermal germ bands 13. Embryos of *L. gigantea* double-labeled for *nodal* and *brachyury*, a gene that is expressed in 3D, mesentoblast 4d, and then very strongly in the distinctly left-right bilateral cells 3d2 and 3c2 14, show that the expression of *nodal* is clearly left-right asymmetric at the 32-64 cell stage and beyond (Figs. 3e-h). Using the *P. vulgata* fate map<sup>15</sup> as a guide, we conclude that *nodal* is expressed in the C quadrant, specifically in the derivatives of the micromeres 1c and 2c. In *P. vulgata*, the progeny of 1c are part of the right cephalic ectoderm of the larvae, whereas 2c-derived cells are part of the ectoderm of the right side of the foot, mantle fold and the shell field 15, suggesting that the two ectodermal domains seen at the larval stages are composed of a subset of the *nodal*-expressing cells from the 64 cell stage. *Pitx* expression was first detected in both snail species at the 64-cell stage in a group of cells of the D quadrant, close to those that express *nodal* (Fig 3 b,d,i and j).

To experimentally investigate the function of Nodal signaling in snail development, we used the chemical inhibitor SB-431542. The TGF- $\beta$  superfamily includes a large number of ligands, but since the drug SB-431542 specifically interferes with type I receptors *alk4*, *alk5*, and *alk7* 16, only the activity of Nodal/Activin/TGF ligands are expected to be blocked by this drug. Of the potential members of the TGF- $\beta$  superfamily that we have identified in the genome of *L. gigantea* (Supplementary Results and Supplementary Fig. 2), only Nodal and Activin signaling should be affected by SB-431542. Given, however, that we have not been able to detect the expression of any of the potential *activin* homologs during embryonic or larval stages, we suggest that SB-431542 treatment might affect exclusively Nodal signaling during snail development prior to the juvenile stage.

Different developmental stages of *B. glabrata* were treated with SB-431542, and the percentages of specific abnormalities varied depending on the concentration and the timing of drug treatment (Supplementary Table 1). By far the most frequently observed phenotype following application of drug at early stages (1-16 cells) was the production of embryos that failed to complete gastrulation and thus could not form juveniles with shells. Some of the embryos that successfully completed gastrulation, however, displayed a striking phenotype - they developed with non-coiled shells (Fig. 4a-g). At 5 $\mu$ M drug concentration, the straight-shelled phenotype was seen in 8% of the animals that managed to complete gastrulation, but at 10 $\mu$ M concentration rose to 43% of those that completed gastrulation. While the shells showed a slight dorsal-ventral curvature, they were tubular with no sign of the left-handed coiling usually seen in *B. glabrata* (Fig. 4a-g). Varying the time of drug application revealed that exposure at the trochophore stage or later yielded animals that were almost always normal, and exposure at the blastula-gastrula stage yielded no coiling defects. Only by

applying the drug prior to the blastula stage could we obtain animals with coiling defects, suggesting that a role in left-right asymmetry might be the earliest function of *nodal* within the embryo (see Supplementary Table 1). Efforts to further narrow the time of drug inhibition by washing off the drug were ineffective, possibly due to the slow diffusion rate of the drug through the egg capsule or a slow reversal of the drug's biochemical effect on the receptors.

We also followed the development of some of the animals with straight shells over the course of several days. We found that these animals continued to enlarge their shells, indeed forming shells that were quite long and robust, but remained straight (Supplementary Fig. 5). To rule out that the lack of shell coiling was simply due to general poor growth, we applied a different chemical inhibitor, rapamycin, a drug that interferes with the cellular metabolic machinery modifying cell growth and proliferation (see Supplementary Methods). Although the treated embryos showed various, sometimes severe, defects in their morphology, the shells that were formed always showed some degree of coiling. Non-coiled shells similar to those recovered with the SB-431542 drug treatment were not detected (Supplementary Table 2).

To test the effects of the SB-431542 drug treatment on the Nodal pathway at the molecular level, we compared the levels of expression of *nodal* and *Pitx* in control and drug-treated embryos. Although no variation in levels of *nodal* expression was detected (both control and drug treated embryos that survived to the trochophore stage showed strong *nodal* expression), in 30% of the treated embryos the level of expression in the asymmetric domain of *Pitx* was greatly reduced (Fig. 4 h-i; Supplementary Table 3) and in 9.5% of the treated embryos asymmetric expression was undetectable (Fig. 4 j-k; Supplementary Table 3). Remarkably, only the asymmetric expression of *Pitx* was affected by the drug treatment, expression levels in the symmetric domains in the stomodeum and gut were unaltered, suggesting separate regulatory elements for these domains of expression, as previously described in deuterostomes 17. These results indicate that *Pitx* is downstream from *nodal* in snails, just as in deuterostomes. However in snails, unlike in deuterostomes, *nodal* does not appear to regulate its own expression. This is consistent with our observation that *nodal* expression in snails is asymmetric from the outset, whereas in vertebrates *nodal* expression is initially symmetric and depends on the regulated feedback of *nodal*-signaling to achieve an asymmetric pattern 2.

The drug treatment results along with our analysis of the expression of *nodal* and *Pitx* provide preliminary support for our contention that Nodal signaling plays a role in left-right asymmetry in snails. The reduction of Nodal signaling leads to a randomization of asymmetry in vertebrates, but it is interesting to note that in snails we observe a lack of asymmetry. Although chirality in snails is first defined at the transition from the 4 to 8-cell stage, the first indication of morphological asymmetry in snails is given by a displacement of the shell gland to the left in dextral species and to the right in sinistral species. We suggest that the asymmetric activity of the Nodal pathway could lead to unequal formation of shell producing cells on the two sides of the embryo, or asymmetrically alter the rate of shell production.

Our results provide new insights into the evolution of body plans and left-right specification in Bilateria. Previous studies suggest that some general mechanisms (at the level of involvement of gap junctions and H<sup>+</sup>/K<sup>+</sup> ATPase activity) contributing to left-right asymmetry are shared between distant phyla 18,19. We hypothesize an even closer linkage. Although *Pitx* orthologs have also been identified in non-deuterostomes such as *D. melanogaster* and *C. elegans*, *Pitx* in these species has not been reported in asymmetrical expression patterns. Our results constitute the first data to suggest that asymmetric expression of *Pitx* might be an ancestral feature of the bilaterians. Furthermore, our data suggest that *nodal* was present in the common ancestor of all bilaterians and that it too may have been expressed asymmetrically. Various lines of evidence indicate that the last common ancestor of all snails had a dextral body 20. If this is true, then our data would suggest that this animal expressed both *nodal* and *Pitx* on the right side. Combined with the fact that *nodal* and *Pitx* are also expressed on the right side in sea urchins 7, 21, this raises the possibility that the bilaterian ancestor had left-right asymmetry controlled by *nodal* and *Pitx* expressed on the right side of the body. While independent co-option is always a possibility, the hypotheses we present can be tested by examining *nodal* and *Pitx* expression and function in a variety of additional invertebrates.

Our data also provide a molecular entry point into understanding chirality in snails. In vertebrates, the actual symmetry breaking event occurs before *nodal* is asymmetrically expressed, and the mechanisms that break symmetry appear to be different between various vertebrate species 2,22-24. Likewise, in snails symmetry must be broken before the 8-cell stage, before *nodal* expression begins. Chirality in snails is determined by a still uncharacterized maternal factor, but once chirality is established, *nodal* and *Pitx* are expressed on one side of the embryo. Future studies that determine how *nodal* expression is regulated will lead us towards an understanding of the actual symmetry breaking event in snails, and examination of the steps downstream of Nodal signaling will provide new insights into the developmental control of complex animal morphologies such as shell coiling.

## Methods

We searched the National Center for Biotechnology Information (NCBI) database of genomic sequences from *L. gigantea* and found 9 potential members of the TGF- $\beta$  superfamily. In addition, examination of the NCBI genomic database of the polychaete annelid *Capitella sp. I* identified a potential ortholog of *nodal*. Phylogenetic analyses included the newly determined deduced amino-acid sequence of Nodal of *L. gigantea*, *B. glabrata*, and *Capitella sp. I*, as well as the Nodal sequences of other deuterostomes and other TGF- $\beta$  superfamily members available from GenBank. Sequence data were analyzed with MacClade version 4.05 OSX, MacVector version 7.2.3, and PAUP\* version 4.0b10. The deduced amino-acid sequences were aligned using Clustal X version 1.62b followed by refinement by eye in an effort to maximize positional homology. Ambiguous alignments and gaps were discarded from further phylogenetic analyses. The aligned amino acid sequence was subjected to Bayesian inference (BI) based methods of phylogenetic reconstruction. ProtTest version 1.3 was used to estimate the evolutionary model that best fit the amino-acid data set. The Akaike information criterion (AIC) implemented in ProtTest selected the WAG

+I+G evolutionary model. BI analyses were performed with MrBayes 3.12 by simulating a Metropolis-coupled Markov chain Monte Carlo (MCMCMC) with four simultaneous chains, each of 2 million generations (sampled every 100 generations) under the WAG+I+G model. Trees sampled before the cold chain reached stationarity (as judged by plots of ML scores) were discarded as “burn-in”. The resulting BI consensus tree was rooted in the midpoint. Robustness of the resulting BI tree was evaluated using Bayesian posterior probabilities (BPPs).

Sexually mature *L. gigantea* were collected in Los Angeles, California during the breeding season and *in vitro* fertilizations were performed according to Gould *et al.* 25. A breeding population of *B. glabrata* is maintained in freshwater tanks at 25°C and embryos and larvae are regularly collected and raised in the lab. Embryos of both species were fixed according to Price and Patel 26. PCR reactions were performed with gene-specific (for *L. gigantea*) and degenerate (for *B. glabrata*) primers sequences (available from the authors upon request). 5' and 3' RACE PCR was performed with Invitrogen RACE reagents. Detailed phylogenetic methods are available in Supplementary Methods. *In situ* hybridizations were performed with digoxigenin and fluorescein-labeled RNA probes as previously described by Price and Patel 26. Nodal inhibition was performed by placing egg masses of *B. glabrata* in freshwater containing 1% DMSO and SB431542 (TOCRIS Bioscience) at a concentration of 5 or 10 µM (diluted from a 1 mM stock of SB431542 in DMSO) and treatment with rapamycin was performed by placing egg masses in freshwater containing 1% DMSO and rapamycin (Eton Bioscience Inc.) at a concentration 10 µM (diluted from a 10 mM stock of rapamycin in DMSO). Control embryos were exposed to 1% DMSO. All controls and drug treated embryos were kept in the dark during the treatment period.

## Supplementary Material

Refer to Web version on PubMed Central for supplementary material.

## Acknowledgements

We thank E. Begovic, E. E. Gonzales, and I. Martínez-Solano for help collecting and fertilizing *L. gigantea*. Ana Almeida helped with the drug experiments. D. R. Lindberg provided the *Busycon pulleyi* specimen. The NIAID Schistosomiasis Resource Center provided adults of *B. glabrata*. We thank M. Levine, D. R. Lindberg, P. Liu, M. Modrell, S. Nichols, M. Protas and J. Rehm for comments on the manuscript and I. Hariharan for suggesting the experiments with rapamycin. CG was sponsored by a postdoctoral fellowship of the Ministerio de Educacion y Ciencia (Spain) and the Center for Integrative Genomics. NHP is an Investigator of the Howard Hughes Medical Institute.

## References

1. Massagué J, Gomis RR. The logic of TGFbeta signaling. *FEBS Lett.* 2006; 580:2811–2820. [PubMed: 16678165]
2. Hamada H, Meno C, Watanabe D, Saijoh Y. Establishment of vertebrate left-right asymmetry. *Nat. Rev. Genet.* 2002; 2:103–113. [PubMed: 11836504]
3. Supp DM, Witte DP, Potter SS, Brueckner M. Mutation of an axonemal dynein affects left-right asymmetry in *inversus viscerum* mice. *Nature.* 1997; 389:963–966. [PubMed: 9353118]
4. Okada Y, et al. Abnormal nodal flow precedes *situs inversus* in *iv* and *inv* mice. *Mol. Cell.* 1999; 4:459–468. [PubMed: 10549278]

5. Morokuma J, Ueno M, Kawanishi H, Saiga H, Nishida H. *HrNodal*, the ascidian nodal-related gene, is expressed in the left side of the epidermis, and lies upstream of *HrPitx*. *Dev. Genes Evol.* 2002; 212:439–446. [PubMed: 12373589]
6. Duboc V, Rottinger E, Besnardeau L, Lepage T. *Nodal* and *BMP2/4* signaling organizes the oral-aboral axis of the sea urchin embryo. *Dev. Cell.* 2004; 6:397–410. [PubMed: 15030762]
7. Duboc V, Rottinger E, Lapraz F, Besnardeau L, Lepage T. Left-right asymmetry in the sea urchin embryo is regulated by nodal signaling on the right side. *Dev. Cell.* 2005; 9:147–158. [PubMed: 15992548]
8. Schilthuizen M, Davison A. The convoluted evolution of snail chirality. *Naturwissenschaften.* 2005; 92:504–515. [PubMed: 16217668]
9. Boycott AE, Diver C. On the inheritance of sinistrality in *Limnaea peregra*. *Proc. R. Soc. Lond. B Biol. Sci.* 1923; 95:207–213.
10. Sturtevant AH. Inheritance of direction of coiling in *Limnaea*. *Science.* 1923; 58:269–270. [PubMed: 17837785]
11. Freeman G, Lundelius J. The developmental genetics of dextrality and sinistrality in the gastropod *Lymnaea peregra*. *Wilhelm Roux Arch. Dev. Biol.* 1982; 191:69–83.
12. Nederbragt AJ, van Loon AE, Dictus WJ. Evolutionary biology: *hedgehog* crosses the snail's midline. *Nature.* 2002; 417:811–812. [PubMed: 12075342]
13. van den Biggelaar JAM, van Loon AE, Damen WGM. Mesentoblast and trochoblast specification in species with spiral cleavage predict their phyletic relations. *Neth. J. Zool.* 1995; 46:8–21.
14. Lartillot N, Lespinet O, Vervoort M, Adoutte A. Expression pattern of *Brachyury* in the mollusc *Patella vulgata* suggests a conserved role in the establishment of the AP axis in Bilateria. *Development.* 2002; 129:1411–1421. [PubMed: 11880350]
15. Dictus WJAG, Damen P. Cell lineage and clonal-contribution map of the trochophore larva of *Patella vulgata* (Mollusca). *Mech. Dev.* 1997; 62:213–226. [PubMed: 9152012]
16. Inman GJ, et al. SB-431542 is a potent and specific inhibitor of transforming growth factor-beta superfamily type I activin receptor-like kinase (ALK) receptors ALK4, ALK5, and ALK7. *Mol. Pharmacol.* 2002; 62:65–74. [PubMed: 12065756]
17. Christiaen L, et al. Evolutionary modification of mouth position in deuterostomes. *Semin. Cell Dev. Biol.* 2007; 18:502–511. [PubMed: 17656139]
18. Nogi T, Yuan YE, Sorocco D, Perez-Tomas R, Levin M. Eye regeneration assay reveals an invariant functional left-right asymmetry in the early bilaterian, *Dugesia japonica*. *Laterality.* 2005; 10:193–205. [PubMed: 16028337]
19. Oviedo NJ, Levin M. Gap junctions provide new links in left-right patterning. *Cell.* 2007; 129:645–647. [PubMed: 17512395]
20. Ponder WF, Lindberg DR. Towards a phylogeny of gastropod molluscs: Analysis using morphological characters. *Zool. J. Linn. Soc.* 1997; 119:83–265.
21. Hibino T, Nishino A, Amemiya S. Phylogenetic correspondence of the body axes in bilaterians is revealed by the right-sided expression of *Pitx* genes in echinoderm larvae. *Dev. Growth Differ.* 2006; 48:587–595. [PubMed: 17118013]
22. Palmer AR. Symmetry breaking and the evolution of development. *Science.* 2004; 306:828–833. [PubMed: 15514148]
23. Duboc V, Lepage T. A conserved role for the Nodal signaling pathway in the establishment of dorso-ventral and left-right axes in deuterostomes. *J. Exp. Zool. B Mol. Dev. Evol.* 2008; 310:41–53. [PubMed: 16838294]
24. Levin M. Left-right asymmetry in embryonic development: a comprehensive review. *Mech. Dev.* 2005; 122:3–25. [PubMed: 15582774]
25. Gould MC, Stephano JL, Ortíz-Barrón BJ, Pérez-Quezada I. Maturation and fertilization in *Lottia gigantea* oocytes: intracellular pH, Ca(2+), and electrophysiology. *J. Exp. Zool.* 2001; 290:411–420. [PubMed: 11550189]
26. Price AL, Patel NH. Investigating divergent mechanisms of mesoderm development in arthropods: the expression of *Ph-twist* and *Ph-mef2* in *Parhyale hawaiensis*. *J. Exp. Zool. B. Mol. Dev. Evol.* 2008; 310:24–40. [PubMed: 17152085]

27. Shibasaki Y, Shimuzu M, Kuroda R. Body handedness is directed by genetically determined cytoskeletal dynamics in the early embryo. *Current Biology*. 2004; 14:1462–1467. [PubMed: 15324662]
28. Camey T, Verdonk NH. The early development of the snail *Biomphalaria glabrata* (Say) and the origin of the head organs. *Neth. J. Zool*. 1970; 20:93–121.

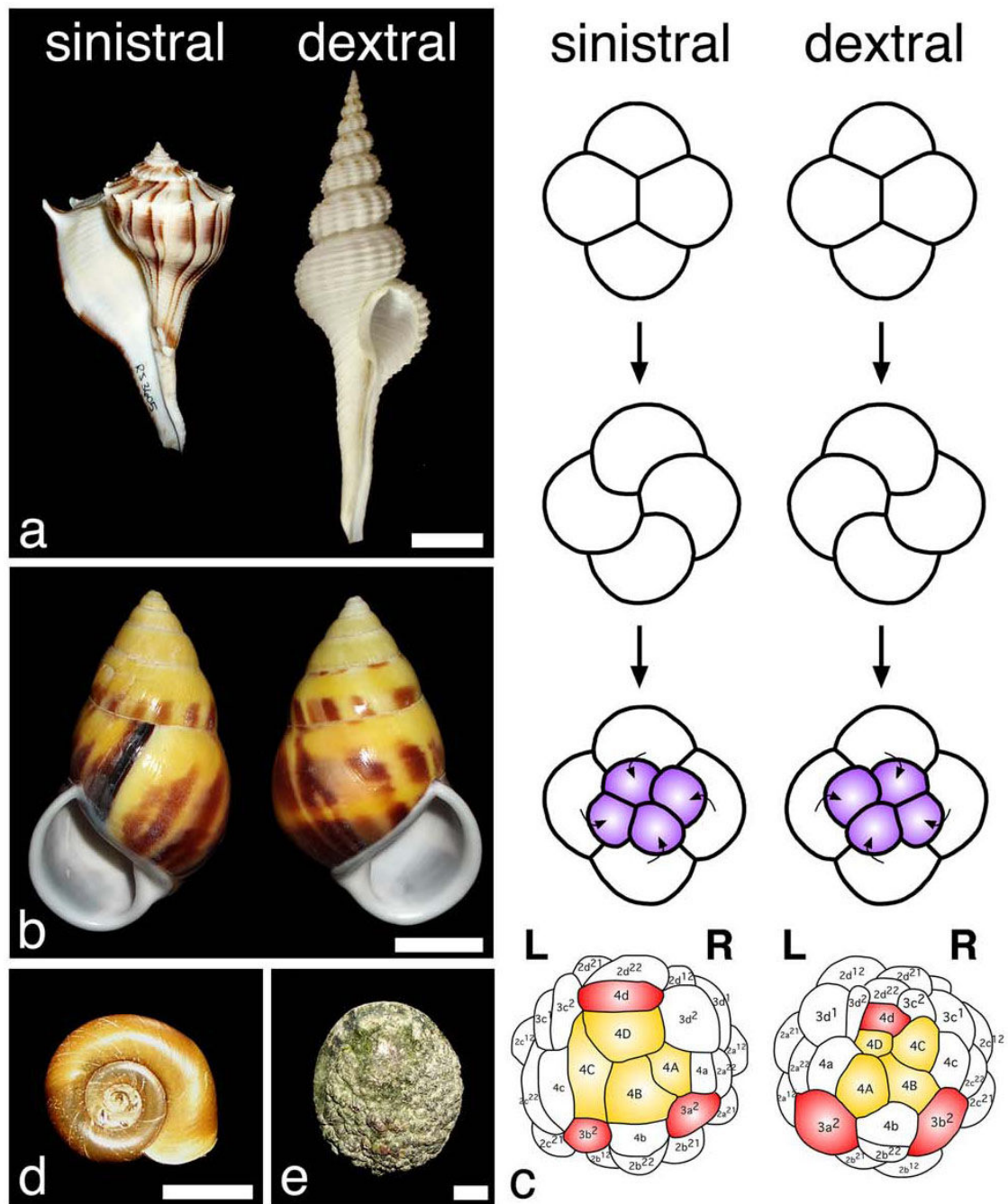


**Figure 1. Chirality in snails**

**a.** Species with different chirality: sinistral *Busycon pulleyi* (left) and dextral *Fusinus salisbury* (right). **b.** Sinistral (left) and dextral (right) shells of *Amphidromus perversus*, a species with chiral dimorphism. **c.** Early cleavage in dextral and sinistral species (based on Shibazaki *et al.* 27). In sinistral species, the third cleavage is in a counterclockwise direction, but clockwise in dextral species. In the next divisions the four quadrants (A, B, C, and D) are oriented as indicated. Cells colored in yellow have an endodermal fate and those in red have an endomesodermal fate in *P. vulgata* (dextral) 15 and *B. glabrata* (sinistral) 28.

**d**, *B. glabrata* possesses a sinistral shell and sinistral cleavage and internal organ organization. **e**, *L. gigantea* displays a dextral cleavage pattern and internal organ organization, and a relatively flat shell characteristic of limpets. Scale bars: 2.0 cm in **a**; 1.0 cm in **b**; 0.5 cm in **d**; 1.0 cm in **e**.

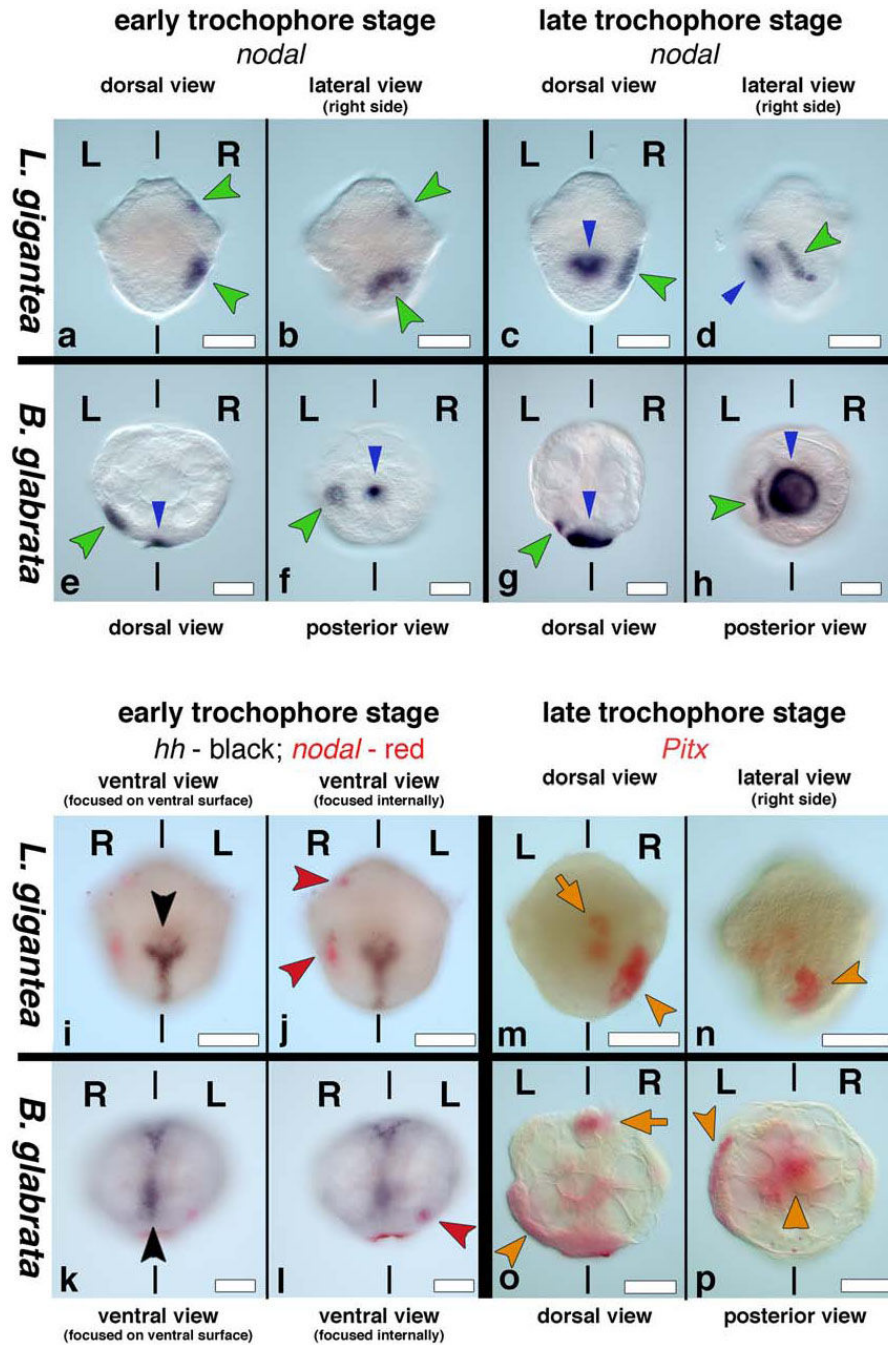


**Figure 2. *nodal* and *Pitx* expression in snails**

Anterior is up, L and R indicate left and right sides. Blue arrowhead in **c-h** indicates non-specific staining of the shell. **a-b**, *nodal* is expressed in the right cephalic region (upper green arrowhead) and right lateral ectoderm (lower green arrowhead) in *L. gigantea* as seen from dorsal (**a**) and right lateral views (**b**). **c**, Expression is maintained in the right lateral ectoderm (green arrowhead); right lateral view (**d**) shows that *nodal* expression (green arrowhead) is near the right side of the developing shell (blue arrowhead). **e-h**, *nodal* is expressed in the left lateral ectoderm (green arrowhead) in *B. glabrata* as seen from dorsal

(e) and posterior views (f); g-h, Expression is maintained in the left lateral ectoderm (green arrowhead); posterior view (h) shows that *nodal* expression (green arrowhead) is near the left side of the developing shell (blue arrowhead). i-l, *hedgehog* (black arrowheads in i and k) is expressed along the ventral midline and *nodal* (red arrowheads in j and l) is expressed on the right side of *L. gigantea* (j) and on the left side of *B. glabrata* (l). m-n, *Pitx* is expressed in the visceral mass (orange arrow) and right lateral ectoderm (orange arrowhead) in *L. gigantea* as seen from dorsal (m) and right lateral views (n). o-p, *Pitx* is expressed in the stomodeum (orange arrow), visceral mass (orange triangle) and the left lateral ectoderm (orange arrowhead) in *B. glabrata* as seen from dorsal (o) and posterior views (p). Scale bars: 50  $\mu$ m in all panels.

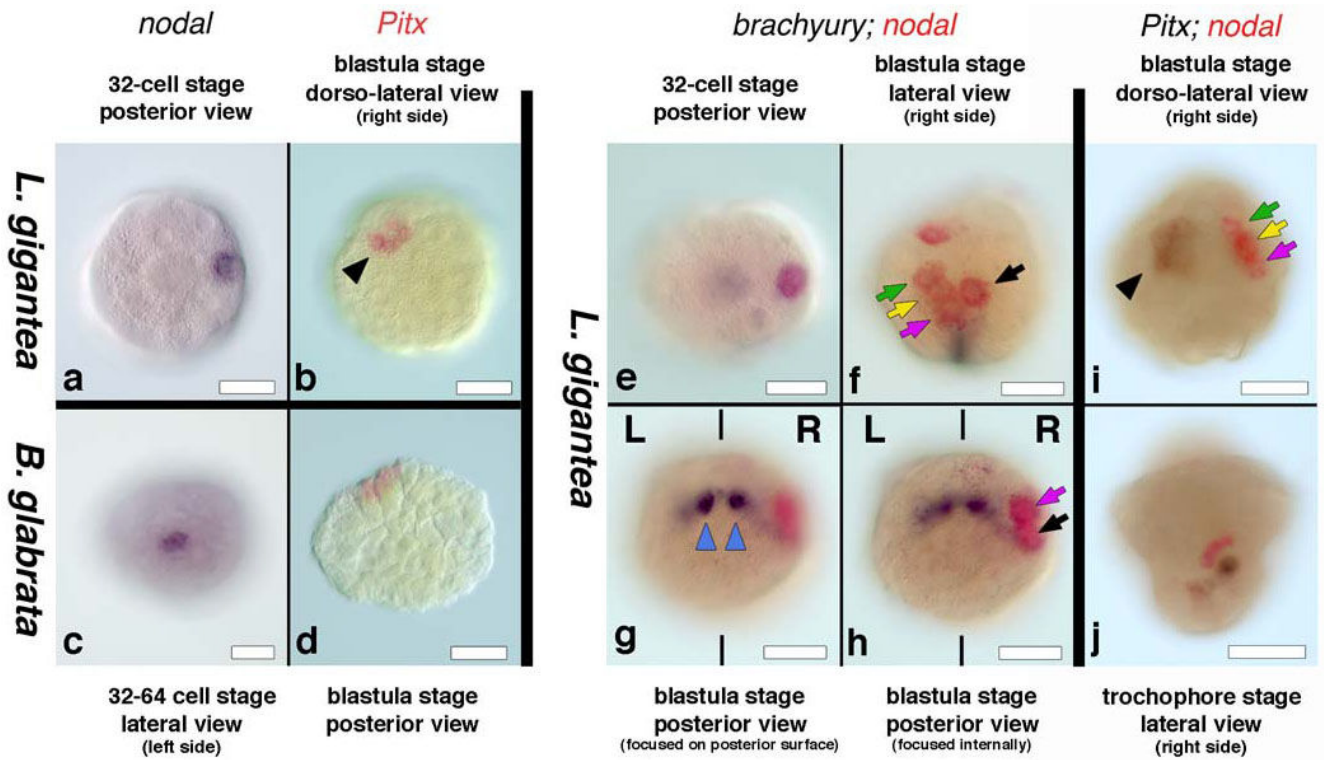


**Figure 3. Early expression of *nodal* and *Pitx* in snails**

**a**, 32-cell stage *L. gigantea* expressing *nodal* in a single cell. **b**, Group of cells expressing *Pitx* in *L. gigantea*. **c**, Onset of *nodal* expression in *B. glabrata*. **d**, Group of cells expressing *Pitx* in *B. glabrata*. **e**, 32-cell *L. gigantea* expressing *nodal* (red) in a single cell (2c) and *brachyury* (black) in two cells (3D and 3c). **f-h**, *brachyury* (black) is expressed in a symmetric fashion in progeny of 3c and 3d blastomeres (blue triangles in **g**), thus marking the bilateral axis and *nodal* (red) is expressed on the right side of *L. gigantea* in the progeny of 2c and 1c blastomeres, as seen from the lateral (**f**) and posterior (**g, h**) views of the same embryo. **i**, Group of cells expressing *nodal* (red) in the C quadrant and *Pitx* (black) in the D quadrant of the 120-cell stage embryo of *L. gigantea*. **j**, *nodal* (red) and *Pitx* (black) expression in adjacent areas of the right lateral ectoderm in *L. gigantea*. L and R indicate the left and right sides of the embryo, respectively. The black triangle in **b** and **i**, the green, yellow, and pink arrows in **f** and **i**, and the black and pink arrows in **f** and **h** point to the equivalent cells. Scale bars: 50  $\mu$ m in all panels.

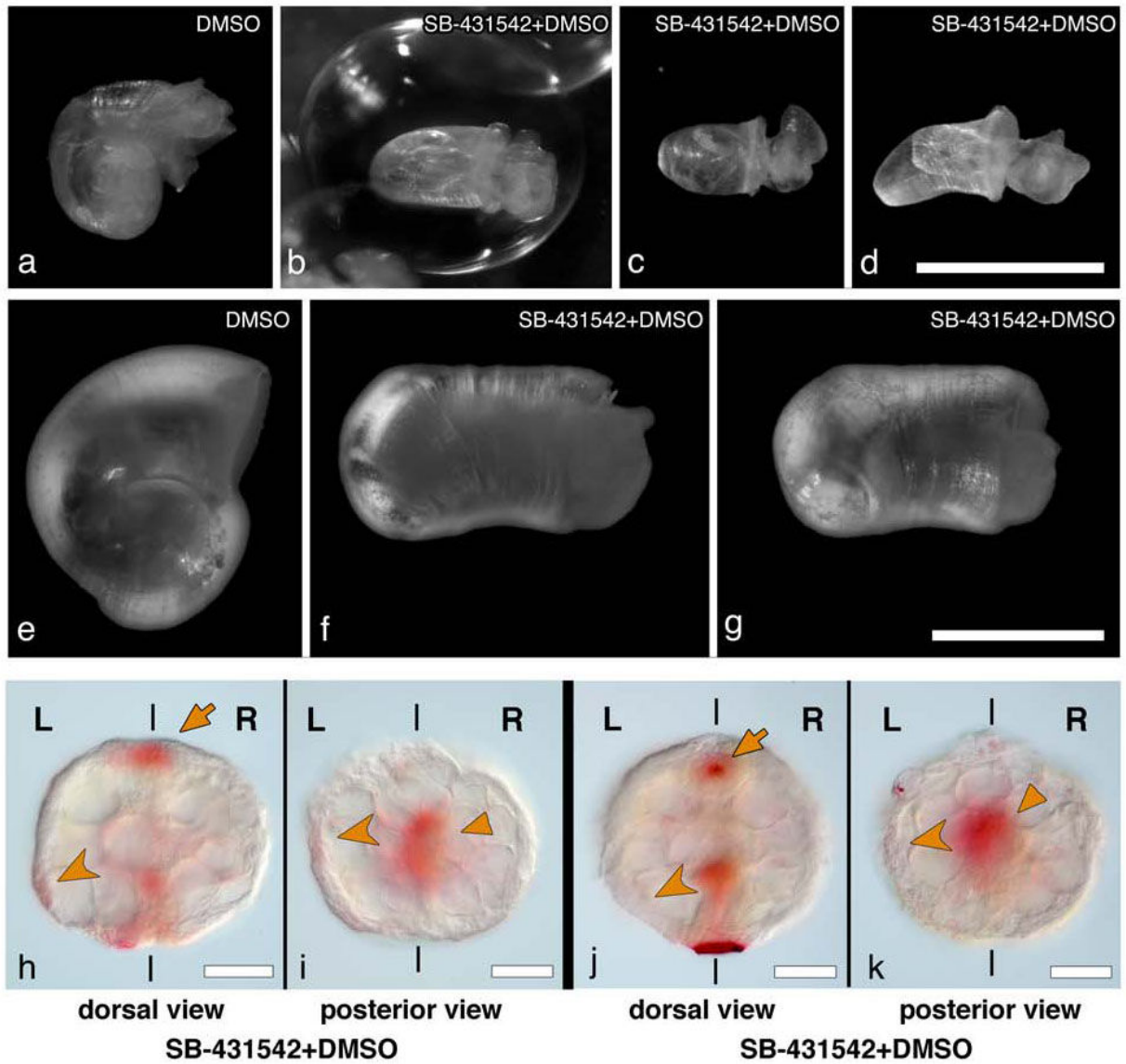


**Figure 4. Wild type coiled and drug-treated non-coiled shells of *B. glabrata* and *Pitx* expression in drug-treated embryos**

Control animals (**a**, **e**) display the normal sinistral shell morphology. Drug treated animals (**b-d**, **f-g**, exposed to SB-431542 from the 2 cell stage onwards) have straight shells. **b-d** are three different living individuals; **f** and **g** are a fourth individual, ethanol fixed, and shown from the side (**f**) and slightly rotated (**g**). **h-k**, *Pitx* expression in embryos exposed to SB-431542. Dorsal (**h**) and posterior views (**i**) of an embryo showing reduced levels of expression. *Pitx* expression is maintained in the stomodeum (orange arrow in **h**) and the visceral domain (orange triangle in **i**), but asymmetric expression in left ectoderm is greatly reduced (orange arrowhead). Dorsal (**j**) and posterior views (**k**) of an embryo in which the asymmetric ectodermal expression of *Pitx* is undetectable (orange arrowhead in **j** and **k** shows where expression would be expected), although the stomodeal (orange arrow in **j**) and visceral domain (orange triangle in **k**) expression of *Pitx* is normal. *Pitx* expression levels shown in **h-k** should be compared to levels in wildtype embryos in figure 2 **o-p**, which are

the same levels seen in DMSO treated animals. L and R indicate the left and right sides of the embryo. Scale bars: 1.0 mm in **a-d**; 0.5 mm in **e-g**; 50  $\mu\text{m}$  in **h-k**.